Available online at www.eccomasproceedia.org
Eccomas Proceedia COMPDYN (2025) 4584-4594

ECCOMAS
Proceedia

COMPDYN 2025
10th ECCOMAS Thematic Conference on
Computational Methods in Structural Dynamics and Earthquake Engineering
M. Papadrakakis, M. Fragiadakis (eds.)
Rhodes Island, Greece, 15-18 June 2025

EVALUATION OF SOIL STRUCTURE INTERACTION EFFECTS ON PEAK FLOOR ACCELERATION PREDICTIONS IN NUCLEAR POWER PLANTS USING RECORDED DATA FROM THE FUKUSHIMA EVENT

Yakub A. Muniru[1], Tadahiro Kishida[1], Elia Voyagaki[1], and Agathoklis Giaralis[1]

[1]Khalifa University
P.O. Box: 127788, Abu Dhabi, UAE
{100060964, tadahiro.kishida, elia.voyagaki, agathoklis.giaralis}@ku.ac.ae

Abstract

The risk of failure of non-structural components and secondary systems (NSCs) during a seismic event is greater in ultra-critical infrastructure, such as nuclear power plants (NPPs). Peak Floor Acceleration (PFA) serves as a key parameter for assessing the seismic demand on NSCs, as these components typically have vibration periods below 0.1 s. Current seismic design standards do not explicitly incorporate soil-structure interaction (SSI) effects in PFA prediction approaches, which may be important for deeply embedded to-the-ground structures like NPPs. To this end, this study quantifies the potential influence of SSI effects in PFA predictions by considering comprehensive acceleration time series from 13 different basement and 22 superstructure locations at 5 different NPP units of the Fukushima plants recorded during the 2011 Tohoku Earthquake event. A random vibration theory (RVT) based estimator is adopted to predict PFA from floor acceleration Fourier amplitude spectra (FASs), determined by filtering FASs from nearby recorded free-field ground motions through transfer functions accounting for SSI effects and the structure. Numerical data-derived SSI and structure transfer functions as well as analytical SSI transfer functions incorporating, for the first in the literature, judicially defined parameters allowing for data-informed calibration are used for PFA estimation. These estimates are compared to the recorded PFAs, demonstrating that kinematic SSI effects are quite important for accurate PFA prediction for the considered NPPs with more than 12m of ground embedment, while the proposed data-driven refinement to standard analytic SSI transfer function models leads to smaller than 1% average prediction error. It is concluded that current simplified PFA prediction equations of seismic design guidelines need to be extended to account for SSI effects in PFA prediction and that such extensions may be achieved by leveraging recorded data from past seismic events.

Keywords: Nonstructural components, soil structure interaction, random vibration analysis, nuclear power plant, peak floor acceleration, analytical data-calibrated transfer functions.

ISSN:2623-3347
Peer-review under responsibility of the organizing committee of COMPDYN 2025.
doi: 10.7712/120125.12759.24645

1 INTRODUCTION

Critical civil engineering structures are complex systems integrating primary load-bearing structural and geotechnical components with various architectural, mechanical, or electrical nonstructural secondary components and systems (NSCs) [1]. These NSCs may experience significant damage during major seismic events. This damage often results in greater seismic losses and consequences compared to those due to damage in the primary load-bearing components [2], particularly in structures containing hazardous materials [3] such as nuclear power plants (NPPs). The maximum forces acting on the NSCs (e.g. electrical cabinets, piping and its support) can be estimated as the product of their mass and anticipated peak accelerations at their center of mass [4]. For stiff NSCs with vibration periods lower than 0.1s, such as those found in NPPs [2, 5, 6], peak floor accelerations (PFAs) is a dependable surrogate of peak acceleration imposed on NSCs [7, 8]. In this regard, accurate prediction of PFAs is important to manage seismic risks in NPPs.

Past studies have proposed various solutions to predict PFAs with differing levels of complexity [9, 10]. In principle, approaches with increased complexity often lead to reduced uncertainty, mostly attributed to uncertainties in high-frequency ground motion predictions due to the natural record-to-record variability, as highlighted by Ghahari *et al*. [9] who examined PFA predictions in tall buildings in Downtown Los Angeles, California. Their study emphasized the importance of regional factors, such as source characteristics, propagation path, and site effects, as these factors significantly affect PFA predictions. Similarly, the Nuclear Regulatory Commission acknowledges the significance of high-frequency ground excitation in PFA predictions [11]. Moreover, soil-structure interaction (SSI) effects [12] may also influence PFA predictions in NPPs, which are commonly deeply embedded in the ground. However, the current seismic codes of practice, including ASCE 7-22, NEHRP 2020, FEMA P-58 2018, and Eurocode 8-2004, do not account for SSI effects in the PFA prediction approaches they offer to practitioners. Thus, there is scope to probe into the influence of SSI effects on PFA predictions in typical NPP structures under region-specific high-frequency ground motion excitation.

To this aim, this study examines the prediction of PFA in Fukushima No. 1 and 2 NPPs during the catastrophic 2011 Tohoku earthquake conditioned on the recorded free-field ground motions. This is pursued by leveraging a comprehensive dataset of recorded acceleration time series at 13 basement/foundation locations and at 22 superstructure/floor locations. Analytical and empirical data-extracted (observed) SSI transfer functions are developed using structural geometries and observed signals, respectively, to incorporate SSI effects into the prediction. PFA predictions using a random vibrations based formulation are compared to the observed PFAs with a view of evaluating the importance of accurately modelling SSI for predicting PFAs for large, deeply embedded structures.

2 CASE STUDY STRUCTURES AND RECORDED EARTHQUAKE DATA

The pursued numerical evaluation of SSI effects on PFA predictions in typical NPPs considers free-field acceleration ground motions together with base slab (foundation level) and superstructure response acceleration time-histories recorded at the Fukushima No.1 and No.2 NPPs during the great 2011 Tohoku earthquake (Japan) [13]. The ground embedment depth of the Fukushima No.1 units is 13m with structures reaching elevations of 65.5m. Figure 1 shows a typical cross-section of one of the two units (unit 6) of Fukushima No.1. Fukushima No.2 comprises four adjacent units with 12m embedment depth and structures of up to 66.5m of height.

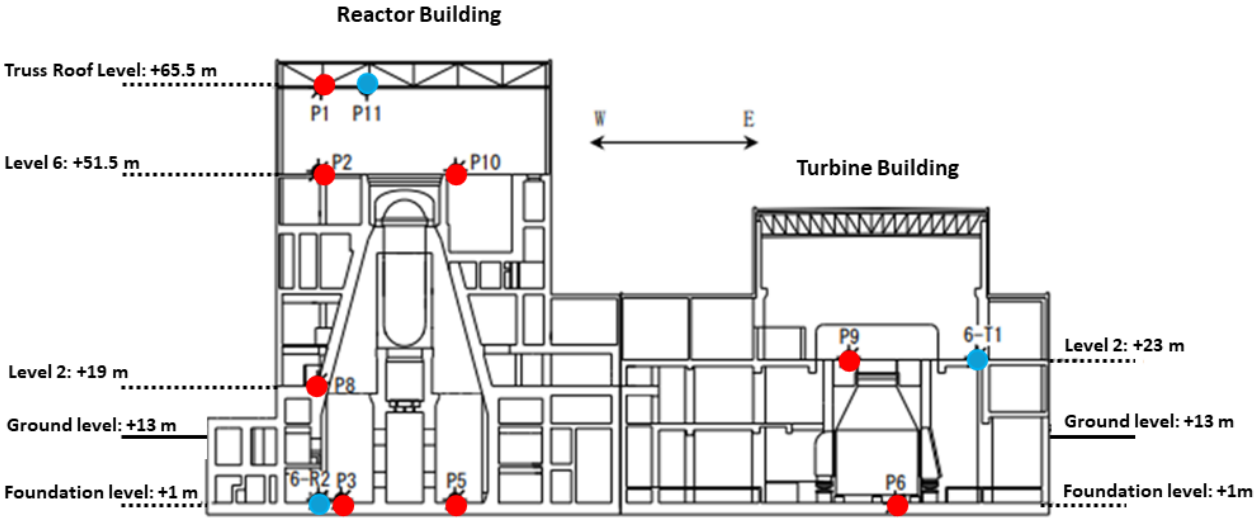

Figure 1: Sectional view of Fukushima No. 1 NPP, Unit 6

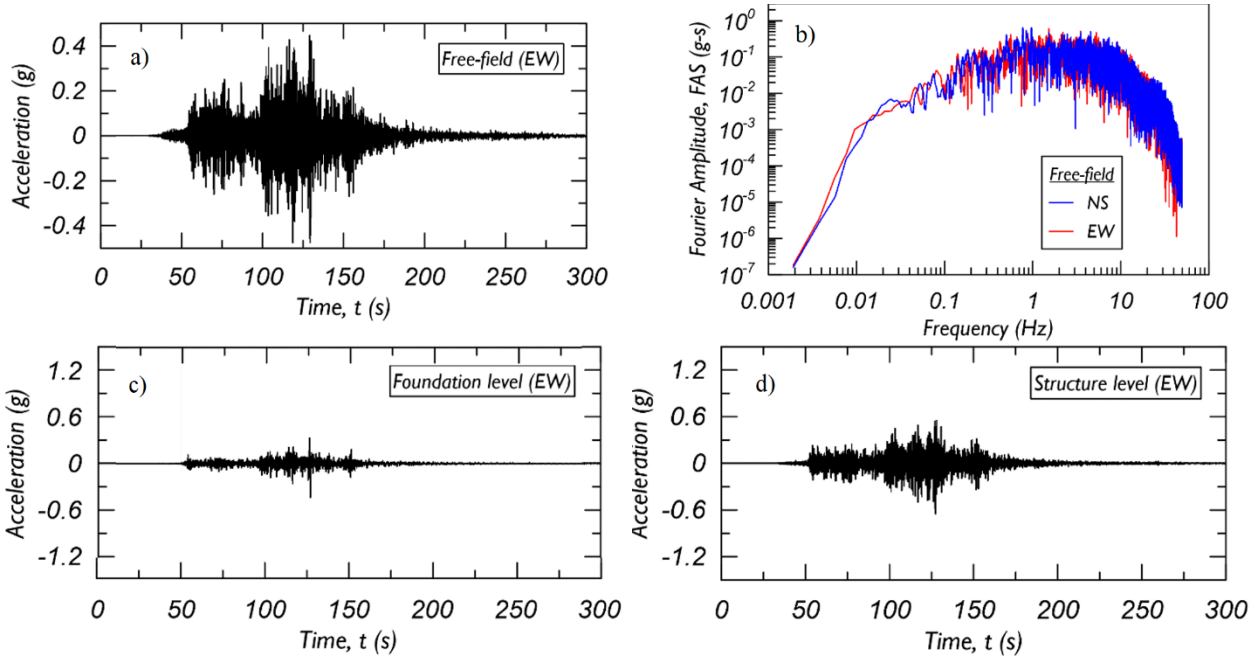

Figure 2: Typical recorded time series for Fukushima No. 1 NPP in Figure 1 E-W direction (a) free field ground motion record (+12.2m elevation), (b) Fourier amplitude spectra of free field records (E-W and N-S directions), (c) foundation level acceleration record at location P3 (+1.0m elevation), (d) structure level acceleration record at location P1 (+65.5m elevation).

Acceleration data from two perpendicular horizontal components recorded at 37 different locations are considered in this study (i.e. a total of 74 time-histories), pertaining to unit 6 of Fukushima No.1, shown in Fig.1, and to all four units of Fukushima No.2 (i.e. 5 NPP units in total). Specifically, free-field ground motions from two different sites are considered, one located at 308m

from unit 6 of Fukushima No.1 and one located at 252m from Fukushima No.2 units. Further, recordings from 13 different locations at the base slab (foundation level) and 22 in-structure locations at different elevations across the 5 units are taken. For illustration, Figure 1 shows the sectional view of Unit 6 Fukushima NPP with red dots denoting the recording locations.

The sampling frequency of all time series is 100 *Hz* with anti-alias filtering at 30 *Hz.* Band-pass Butterworth filters were applied to all recordings according to the approach described in [14]. The median corner frequency for the applied high-pass filter was about 0.03 *Hz* based on signal-to-noise ratio, with the minimum and maximum values ranging from 0.004 to 1.4 *Hz*. Combining the sensor responses with the applied filters makes the recorded signals generally usable in the frequency range of 0.03 Hz to 24 Hz. Figure 2 plots typical time series from the considered dataset.

3 DATA-DRIVEN RANDOM VIBRATION-BASED PFA PREDICTION

The use of random vibration theory (RVT) for estimating the expected absolute peak time-domain values from Fourier amplitude spectra (FAS) of non-stationary time series is common in earthquake engineering and has been proved reasonably accurate in a number of applications (e.g. [10, 15-17]). For the purposes of this work, RVT is the approach of choice as it enables to explicitly account for SSI effects in estimating the PFA at each of the 22 Fukushima NPP structure recording locations through a straightforward frequency-domain treatment of the problem. Specifically, the RVT-based estimator of PFA is given as

$$PFA_{est} = \eta_p \sqrt{\frac{1}{\pi D}\int_0^{\omega_{max}} \left|\ddot{Y}(\omega)\right|^2 d\omega} \tag{1}$$

where $\left|\ddot{Y}(\omega)\right|$ is the FAS of the seismic response acceleration time series at the in-structure location (floor) of interest, D is an effective duration of this time series, ω_{max} is a cut-off frequency above which the FAS is not usable (e.g. due to data reliability or due to insignificant FAS values), and η_p is the so-called peak factor of RVT. In the herein discussed setting, the latter is rigorously defined as the factor by which the standard deviation of the acceleration time series, modelled as a quasi-stationary random process, must be multiplied to predict the threshold below which the PFA will remain with probability p, throughout the duration D (e.g. [18]).

Herein, p is taken equal to 0.5 to achieve a median value estimator in Eq.(1) [19], and the peak factor formulation due to Der Kiureghian [20] is adopted to compute $\eta_{p=0.5}$ as implemented in the pyRVT open software [21]. Further, following [17], the duration D is adjusted as a means to compensate for the non-stationary nature of the floor acceleration time series, which violates the quasi-stationary assumption invoked by Eq.(1), through the expression

$$D = D^* \left(\frac{PFA^*_{est}}{PFA_{obs}}\right)^2 \tag{2}$$

where D^* is a seed duration value, PFA^*_{est} is the PFA estimated from Eq.(1) by using D^*, and PFA_{obs} is the PFA derived from the recorded floor acceleration time series (observed) presented in the previous section. Lastly, the acceleration FAS in Eq.(1) is derived separately for the two horizontal directions (N-S and E-W) at each structure location by frequency-domain filtering of the FAS of the corresponding free-field ground motions at the geotechnical downhole array, $\left|\ddot{U}_g(\omega)\right|$ (see e.g. Figure 2(b)), through one transfer function that accounts for the SSI effects,

$TF_{SSI}(\omega)$, and a second transfer function that accounts for the structure, $TF_{str}(\omega)$, using the expression

$$\left|\ddot{Y}(\omega)\right| = |\,TF_{str}(\omega)||\,TF_{SSI}(\omega)|\,\left|\,\ddot{U}_g(\omega)\right| \tag{3}$$

The FAS $\left|\,\ddot{U}_g(\omega)\right|$ is computed from the entire free field ground acceleration time series. The structure transfer functions are derived for each one of the 22 structure locations along the N-S and E-W directions using standard input-output linear system identification (e.g. [22]), whereas the entire structure acceleration times series is used as output signal and the entire acceleration time series from foundation location immediately below each structure locations is used as input signal. For illustration, Figure 3 plots the TF_{str} for P1 location in Figure 1 along N-S and E-W directions, using recorded acceleration time series from P1 (output) and P3 (input) locations. As seen in Figure 3, the thus obtained (observed) transfer functions are quite jagged, therefore a log-frequency rectangular window with a width of 0.05 in $\log_{10}$ scale was used to extract smooth structure transfer functions which are used in Eqs.(1)-(3) for PFA predictions. Notably, the consideration of these data-driven structure transfer functions facilitates the investigation of the influence of the SSI transfer function in Eq.(3) which is the main focus of this work. To this aim, both theoretical parametric models and data-driven transfer functions are used in place of TF_{SSI} in Eq.(3) to draw comparisons, as detailed in the following section.

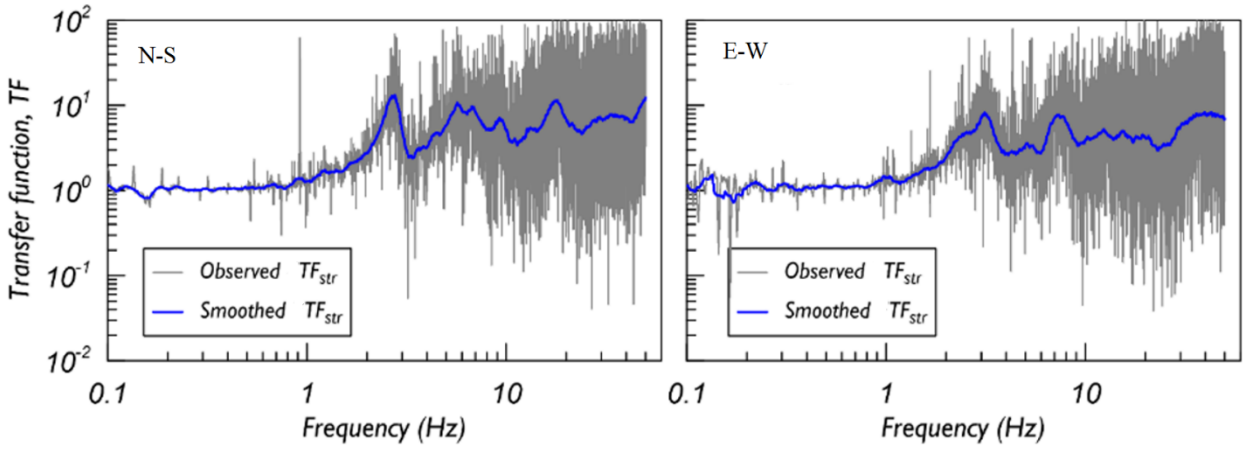

Figure 3: Structure transfer functions for Fukushima No 1 NPP between P3 foundation location and P1 structure (roof) location (N-S and E-W directions).

4 SOIL-STRUCTURE-INTERACTION MODELLING

The importance of inertial SSI effects depends on the structure-to-soil stiffness ratio (e.g. [23]). This ratio is lower than 0.1 for the case study Fukushima No. 1 and No. 2 NPPs; therefore, inertial SSI effects are negligible compared to the kinematic SSI effects, based on the [12]. In this regard, the TF_{SSI} component in Eq.(3) is herein modelled analytically to represent only kinematic SSI effects, namely base slab averaging (BSA) and embedment (e.g. [24]) as

$$|\,TF_{SSI}(\omega)| = \left|\,TF_{SSI}^{BSA}(\omega)\right|\left|\,TF_{SSI}^{embed}(\omega)\right| \tag{4}$$

where

$$\left| TF_{SSI}^{BSA}(\omega) \right| = \begin{cases} \left(\dfrac{\sin\left(\alpha\omega B/V_{app}\right)}{\alpha\omega B/V_{app}} \right)^{\beta}, & \dfrac{\omega B}{V_{app}} \le \dfrac{\pi}{2} \\ \left(\dfrac{2}{\pi}\right)^{\beta}, & \dfrac{\omega B}{V_{app}} > \dfrac{\pi}{2} \end{cases} \tag{5}$$

and

$$\left| TF_{SSI}^{embed}(\omega) \right| = \begin{cases} \left(\cos\left(\alpha \dfrac{e\omega}{V_s}\right) \right)^{\beta}, & \alpha \dfrac{e\omega}{V_s} \le 1.1 \\ (0.454)^{\beta}, & \alpha \dfrac{e\omega}{V_s} \ge 1.1 \end{cases} \tag{6}$$

In Eq.(5), B is half the foundation width along the excitation direction and $V_{app} = V_s/\sin i$ is the apparent seismic shear wave velocity propagation with V_s being the shear wave velocity and i the angle of incidence of the seismic waves. The latter is estimated as $i \approx 18°$ following [25] and using the recorded signals. Further, in Eq.(6), e is the embedment depth. Moreover, α and β in Eqs. (5) and (6) are newly introduced coefficients which govern the corner frequency value above which $|TF_{SSI}(\omega)|$ model in Eq.(4) reduces, and the constant value of $|TF_{SSI}(\omega)|$ at high frequencies, respectively. For α=β=1, Eqs.(5) and (6) coincide with the SSI models for BSA and embedment found in the literature (see [24] and references therein). In this respect, coefficients α and β are herein used to modify the analytical $|TF_{SSI}(\omega)|$ model in Eq.(4) to achieve a better matching with the observed SSI transfer functions, $\left|TF_{SSI}^{obs}(\omega)\right|$. The latter functions are derived from the Fukushima time series at 13 basement level locations (two per location along E-W and N-S directions), using the same system identification approach and smoothing as in the case of the observed structure transfer function discussed in the previous section.

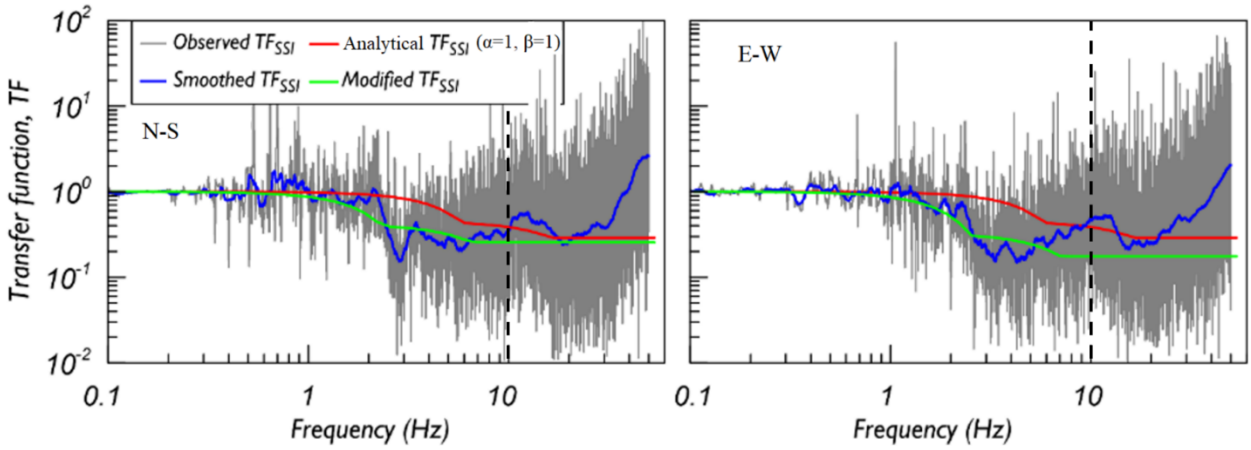

Figure 4: SSI Transfer functions for Fukushima No 1 NPP between P3 foundation location and free field ground motion (N-S and E-W directions).

Representative analytical and observed SSI transfer functions are plotted in Figure 4 for the P3 basement location in Figure 1 (similar trends hold for the other 12 locations). It is seen that the analytical unmodified $|TF_{SSI}(\omega)|$ model in Eq.(4) with α=β=1 matches well the data-derived

smoothed SSI transfer functions, extracted from the overly noisy observed transfer functions, $\left| TF_{SSI}^{obs}(\omega) \right|$, within a band of 0.1 Hz to 2 Hz. For frequencies above 2 Hz, the level of matching deteriorates which motivated the introduction of the α and β modification coefficients in the analytical SSI transfer function. Indeed, the modified (analytical) transfer functions obtained by varying α and β based on the data-driven smoothed SSI transfer functions (corner period and high-frequency transfer function ordinate) match closely the smoothed SSI transfer function within a much wider frequency band. As a final remark of this section, it is noted that the observed transfer functions (SSI and structure) above 10 Hz are not reliable as the coherence function (ratio of input/output cross-spectrum squared over product of input and output auto-spectra) drops below 0.6 at frequencies above 10 Hz [22]. Therefore, PFA estimation based on Eq.(1) should be made using frequencies up to 10 Hz (or ω_{max}= 62.8 rad/s) as indicated by the black broken line in Figures 3 and 4.

5 COMPARISONS OF PREDICTED PFAS VERSUS RECORDED PFAS

This section compares PFAs predicted from Eq.(1) using 5 different set of assumptions (M1-M5) versus PFAs extracted (observed) directly from the structure acceleration records for all 22 locations with two directions each (i.e. 44 data points in total). The comparisons are shown in Figure 5 and are used first to validate the accuracy of the RVT-based PFA prediction methodology of section 3 and second to quantify the influence and relative importance of SSI effects in PFA prediction for NPPs. Specifically, M1 predictions in Figure 5(a) are made using smoothed data-driven structure and SSI transfer functions including frequencies above 10 Hz in conjunction with duration D from the structure-level recorded time series. The prediction errors are less than 1% for all locations and directions, validating the accuracy and applicability of the RVT-based estimator in Eq.(1) for PFAs. Next, M2 PFA predictions in Figure 5(a) use the same data-derived transfer functions as M1 predictions but with duration D in Eq.(2) calculated from free-field ground motion time series using Eq.(1) estimator with $\left| \ddot{U}_g(\omega) \right|$ FAS to predict peak ground acceleration (PGA). On average, M2 exhibits an average overprediction of PFAs by 3.4%, indicating that duration is important for accurate RVT-based PFA predictions, as heavily discussed in the literature (see e.g. [26] and references therein). Importantly, the deterioration of M2 prediction vis-à-vis M1 indicate that duration in Eq.(1) should be based on structural response acceleration time series instead of ground motion time series. Still, recognizing that in-structure recordings are very rarely available (making the denominator in Eq.(2) elusive), while PGA is the most common ground motion property in seismic design, duration D based on the ground motion time series are adopted in all subsequent PFA predictions.

To this effect, M3 predictions in Figure 5(b) use the same duration and data-derived transfer functions as M2 prediction, but the latter are limited to 10 Hz. The level of accuracy of M2 and M3 predictions is fairly similar to M3, underpredicting PFAs by 2.6% on average, which suggests that high-frequency content above 10 Hz with very low coherency is not important for PFA estimation. Next, M4 predictions in Figure 5(c) are obtained the same way as M3 with only difference being that the analytical unmodified SSI transfer function in Eq. (4) is used with $\alpha = \beta = 1$ instead of the data-derived one. This change significantly deteriorates the quality of the predictions (average overprediction reaches 27%), suggesting that, on the one hand, SSI effects are important for accurate PFA prediction and, on the other hand, the standard analytical SSI models as the ones in Eqs.(5) and (6) are inadequate for capturing faithfully the SSI effects at least for the herein

considered case study NPPs and recorded data. Finally, M5 predictions use the modified analytical SSI transfer functions compared to M4 predictions with α and β coefficients calibrated against the data-driven SSI transfer functions. Excellent agreement is noted between observed and M5 predictions, with the average error level being similar to the M1 predictions (less than 1%) and all predicted PFA values lying within the ±20% error range. These results demonstrate that the herein proposed modified analytical SSI models can effectively replace the data-driven SSI transfer functions and that the influence of the SSI effect on PFA prediction may be more significant than the effective duration used in RVT-based estimation.

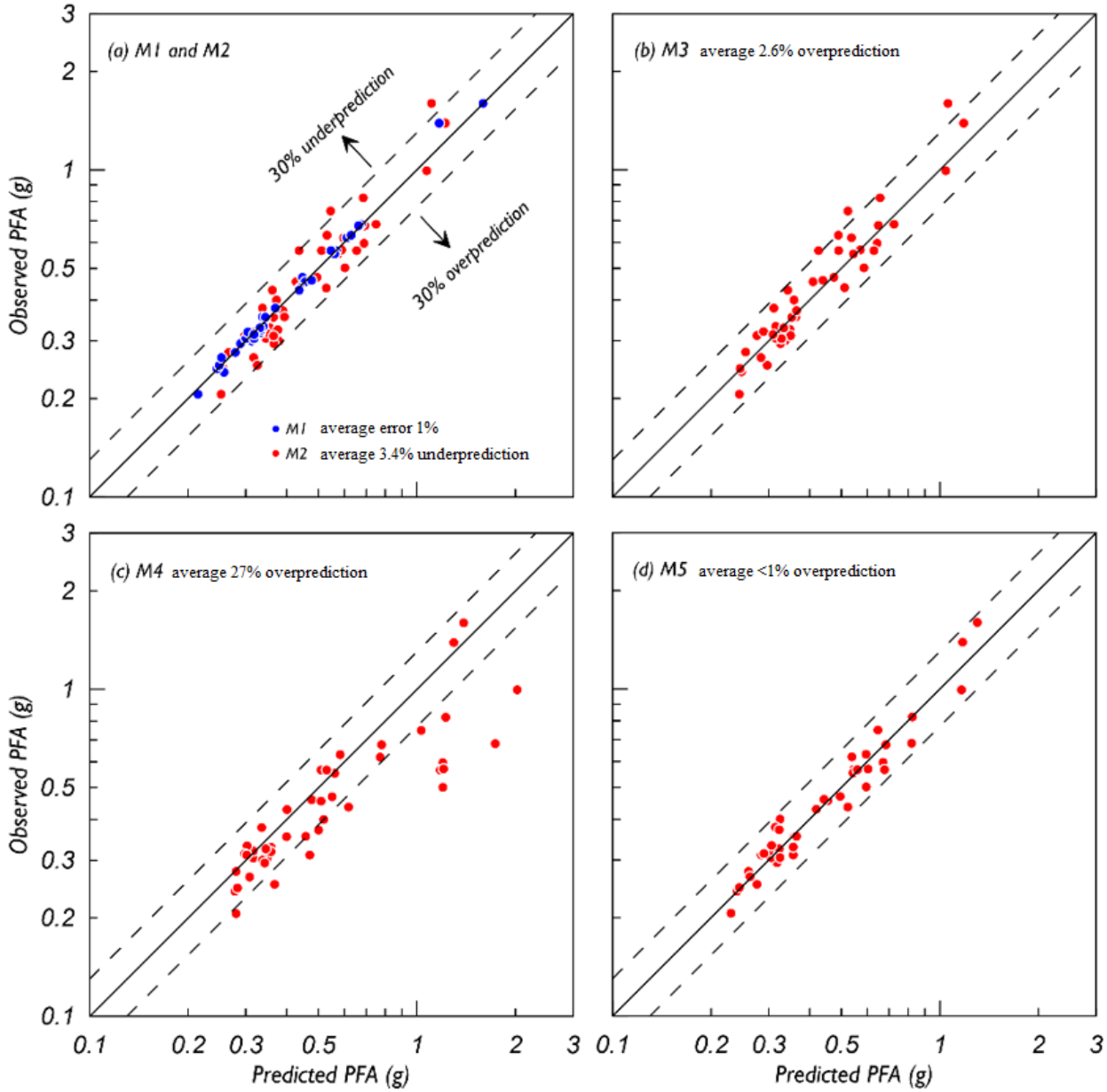

Figure 5: Comparison of predicted PFAs using different assumptions (M1-M5) with observed PFAs from records at 22 structure locations of Fukushima No1 and No2 NPPs, along two horizontal directions per location.

6 CONCLUSIONS

This study investigated the influence of SSI effects on the PFA in typical NPPs whose prediction is critical for assessing the seismic demands and vulnerability of acceleration-sensitive NSCs. This was achieved by considering comprehensive recorded acceleration data along two horizontal perpendicular directions from 13 different basement and 22 superstructure locations of 5 different NPP units of Fukushima plants during the 2011 Tohoku Earthquake event, as well as from nearby free field ground motion records. A random vibration theory (RVT) based estimator was adopted, relying on the concepts of the peak factor and effective duration, to predict PFA from floor acceleration Fourier amplitude spectra (FASs) at the 22 considered in-structure locations. The latter FASs were determined by filtering free-field ground motion FASs through transfer functions accounting for SSI effects and the structure. Numerical data-derived SSI and structure transfer functions as well as analytical parametrically defined SSI transfer functions incorporating for the first in the literature judicially defined parameters allowing for data-informed calibration were used for PFA estimation. These estimates were compared to PFAs directly observed from acceleration recordings along two independent directions at the 22 in-structure locations (i.e. 44 data points in total). Major conclusions from these comparisons are: (i) Kinematic SSI effects are more important for accurate RVT-based PFA prediction than the assumed effective duration of the underlying quasi-stationary random floor acceleration process and (ii) the proposed data-driven refinement to the standard analytic SSI transfer function models is very effective in accurate PFA prediction leading to smaller than 1% average error from 44 samples. Conclusion (i) calls for refinement of current seismic design guidelines, which do not explicitly incorporate SSI effects in PFA prediction approaches, especially for deeply embedded to-the-ground structures like NPPs, while conclusion (ii) suggests that in the current era of data-centered/driven approaches such refinements should leverage recorded data from past seismic events, which further highlight a need for more widespread structural monitoring systems in high seismicity areas.

ACKNOWLEDGEMENTS

The first author is supported by a Khalifa University Combined Master's/Doctoral Research/Teaching Scholarship (CMDRTS). The authors are grateful to TEPCO for sharing the recorded ground motions at Fukushima No.1 and 2 NPPs and to Prof. George Mylonakis for his valuable guidance on the SSI part of this work.

REFERENCES

[1] E. M. Hassan and H. Mahmoud, "A framework for estimating immediate interdependent functionality reduction of a steel hospital following a seismic event," *Eng. Struct.*, vol. 168, pp. 669–683, 2018.

[2] H. Son, S. Park, B. G. Jeon, W. Y. Jung, J. Choi, and B. S. Ju, "Seismic qualification of electrical cabinet using high-fidelity simulation under high frequency earthquakes," *Sustainability*, vol. 12, no. 19, pp. 1–14, 2020.

[3] E. A. Fierro, E. Miranda, and C. L. Perry, "Behavior of nonstructural components in recent earthquakes," in *AEI 2011: Building Integrated Solutions*, 2011, pp. 369–377.

[4] A. Filiatrault, D. Perrone, R. J. Merino, and G. Michele, "Performance-Based Seismic Design of Nonstructural Building Elements," *J. Earthq. Eng.*, vol. 25, no. 2, pp. 237–269,

2021.
[5] S. Kwag *et al.*, "Shaking Table Test and Numerical Analysis of Nuclear Piping under Low- and High-frequency Earthquake Motions," *Nucl. Eng. Technol.*, 2022.
[6] Electric Power Research Institute (EPRI), "High Frequency Program, Application Guidance for Functional Confirmation and Fragility Evaluation," Palo Alto, USA, 2015.
[7] ASCE/SEI 7-16, *Minimum design loads for buildings and other structures*, no. 7–10. Reston, Virginia: American Society of Civil Engineers, 2017.
[8] FEMA P-58-1, "Seismic Performance Assessment of Buildings," *Appl. Technol. Counc. Fed. Emerg. Manag. Agency*, vol. 1, no. December, 2018.
[9] S. F. Ghahari, A. Baltay, M. Çelebi, G. A. Parker, J. J. McGuire, and E. Taciroglu, "Earthquake Early Warning for Estimating Floor Shaking Levels of Tall Buildings," *Bull. Seismol. Soc. Am.*, vol. 112, no. 2, pp. 820–849, 2022.
[10] I. Zentner, "Use of RVT for the Computation of In-Structure Response Spectra and Peak Responses and Comparison to Time History And Response Spectrum Analysis," *Earthq. Spectra*, vol. 34, no. 4, pp. 1913–1930, 2018.
[11] J. Hur and A. Shafieezadeh, "Performance of nonstructural components in NPPs under high-frequency ground motions," *13th Int. Conf. Appl. Stat. Probab. Civ. Eng. ICASP 2019*, pp. 1–8, 2019.
[12] FEMA, "A Practical Guide to Soil-Structure Interaction," Report P-2091, Applied Technology Council, Washington, D.C., 2020.
[13] Architectural Institute of Japan and Tohoku Branch Disaster Investigation Committee, "Ground motion database in Tohoku region during 2011 Tohoku earthquake," 2013. [Online]. Available: Ver.1.0 (CD-ROM)
[14] C. A. Goulet *et al.*, "PEER NGA-East database," *Earthq. Spectra*, vol. 37, no. 1, pp. 1331–1353, 2021.
[15] P. D. Spanos, A. Giaralis, and L. Jie, "Synthesis of accelerograms compatible with the Chinese GB 50011-2001 design spectrum via harmonic wavelets : artificial and historic records," *Earthq. Eng. Eng. Vib.*, vol. 8, no. 2, pp. 189–206, 2009.
[16] C. Van Houtte, T. Larkin, and C. Holden, "On durations, peak factors, and nonstationarity corrections in seismic hazard applications of random vibration theory," *Bull. Seismol. Soc. Am.*, vol. 108, no. 1, pp. 418–436, 2018.
[17] D. M. Boore and E. M. Thompson, "Empirical improvements for Estimating earthquake response spectra with random-vibration theory," *Bull. Seismol. Soc. Am.*, vol. 102, no. 2, pp. 761–772, 2012.
[18] E. H. Vanmarcke, "Structural Response to Earthquakes," in *Lomnitz C and Rosenblueth E, Seismic Risk and Engineering Decisions*, vol. 15, Amsterdam: Elsevier, 1976, pp. 287–337.
[19] A. Giaralis and P. D. Spanos, "Effective linear damping and stiffness coefficients of nonlinear systems for design spectrum based analysis," *Soil Dyn. Earthq. Eng.*, vol. 30, no. 9, pp. 798–810, 2010.
[20] A. Der Kiureghian, "Structural response to stationary excitation," *J. Eng. Mech. Div.*, vol. 106, no. 6, pp. 1195–1213, 1980.
[21] A. Kottke, "pyRVT Documentation," 2020, [Online]. Available: https://doi.org/10.5281/zenodo.3630729
[22] A. Mikami, J. P. Stewart, and M. Kamiyama, "Effects of time series analysis protocols on transfer functions calculated from earthquake accelerograms," *Soil Dyn. Earthq. Eng.*, vol.

28, no. 9, pp. 695–706, 2008.
[23] J. P. Stewart, R. B. Seed, and G. L. Fenves, "Seismic Soil-Structure Interaction in Buildings. II: Empirical Findings," *J. Geotech. Geoenvironmental Eng.*, vol. 125, no. 1, pp. 38–48, 1999.
[24] G. Mylonakis, S. Nikolaou, and G. Gazetas, "Footings under seismic loading: Analysis and design issues with emphasis on bridge foundations," *Soil Dyn. Earthq. Eng.*, vol. 26, no. 9, pp. 824–853, 2006.
[25] M. J. O'Rourke, M. C. Bloom, and R. Dobry, "Apparent Propagation Velocity of Body Waves," *Earthq. Eng. Struct. Dyn.*, vol. 10, pp. 283–294, 1982.
[26] M. K. Kolli and S. S. Bora, "On the use of duration in random vibration theory (RVT) based ground motion prediction: a comparative study," *Bull. Earthq. Eng.*, vol. 19, no. 4, pp. 1687–1707, 2021.